Pis'ma v ZhETF, vol.68, iss.6, pp.442 - 448

THEORY OF SONOLUMINESCENCE IN SINGLE BUBBLES: FLEXOELECTRIC ENERGY CONTRIBUTION

N.García[+], *A.Hasmy*[+*]

[+]*Laboratorio de Física de Sistemas Pequeños y Nanotecnología, CSIC*
28006 Madrid, Spain

[*]*Laboratorio de Física Estadística de Sistemas Desordenados, Centro de Física, IVIC,*
Apartado 21827, Caracas 1020A, Venezuela

Submitted 10 August, 1998

We introduce an equation of motion for a cavitating gas bubble immersed in a liquid which includes a flexoelectric energy term. This energy is deduced from the electric field produced by the bubble wall acceleration (pressure gradient) in the fluid (flexoelectric effect). We show that, in sonoluminescence conditions, this electric field reaches values of typical electric breakdown in water. Our theoretical results is consistent with duration of light emission, bubble minimum radius and released energy as measured in sonoluminescence experiments in water.

PACS: 78.60.Mq, 47.55.Bx, 52.80.-s

A short and intense flash of light is emitted when ultrasound-driven air (or other gas) bubbles immersed in a liquid collapse. This phenomenon, discovered 60 years ago [1], is called *sonoluminescence* (SL). Renewed interests exist now because a crucial experiment [2] showed repetitive emissions from a single, stable cavitating gas bubble in water. Usually, SL experiments address a range of parameter values where the emission is stable, since it has been shown [3] that the existence of SL and its stability depend on parameter conditions. A variety of interesting measurements have been reported in the literature, namely the evolution of the bubble radius R [2-5], the spectrum of the emitted light [6] and the effect of noble gas doping in single bubble [7, 8]. Measurements indicate that the released energy is $\sim 10^{-12}$ J [6] and the duration of light emission ranges from 40 ps to over 350 ps[8].

From the theoretical point of view, the pioneering work for the equation of motion of a cavitating bubble is due to Rayleigh [9]. Later, the Rayleigh equation has been generalized by taking into account the compressibility, surface tension and the viscosity of the fluid. Additionally, an acoustic pressure term has been added to describe bubble cavitation experiments under the action of this acoustic field. All these considerations lead to the Rayleigh-Plesset (R-P) equation [10]. Even if this equation has been used with success to describe the evolution of the radius of a cavitating bubble, its fails when one tries to reproduce in detail the evolution of the radius of SL experiments in the region where light emission occurs (i.e. near to the bubble collapse); neither the SL phenomenon, nor the light emission mechanism is explained by this theory. Recently, García and Levanyuk [11] proposed a new hypothesis which takes into account the fact that in SL experiments high pressure gradients produce high electric fields due to the flexoelectric effect [12]. This effect has been invoked previously to explain polarization of water by shock waves [13]. The estimated time of the shock action is 1 ps, while the relaxation time of the water polarization at 25 °C is 9 ps [14], and the mechanism of polarization in the shock wave can be quite different from the dipole orientation mechanism which dominates for intervals longer than the relaxation time. In the SL case the typical time for buildup of large pressure gradients is 10^{-9} s, a time much larger than the breakdown time.

As predicted by García and Levanyuk [11], this letter show that, for parameters where SL has been observed experimentally, the collapsing region of the bubble produces electric fields of the same order of the electric breakdown field E_{bd} in water (which has an electronic character, being $\sim 10^7$ V/m in static conditions [15] and $\sim 10^8$ V/m in dynamic conditions [16]). Furthermore, as we will show below, when the flexoelectric potential energy is accounted for, in this collapsing region, the radius evolution of the bubble agrees with a recent experiment; in particular, the minimum radius R_m whit measured values in many experiments (0.7 μm) [4, 5]. Calculations of the released energy and duration of the emission are also consistent with experimental results [5, 8].

Including up to first order corrections due to the fluid compressibility (as proposed by Herring [17]), energy conservation for the bubble reads:

$$2\pi\rho_w R^3(1-\frac{4}{3}\frac{\dot{R}}{c_w})\dot{R}^2+U=$$
$$=\int_{R_o}^{R}[P_g-P_a-P_o+\frac{R}{c_w}\frac{d}{dt}(P_g-P_a)-\frac{2}{R}(\sigma+2\nu\dot{R})]4\pi R^2 dR, \qquad (1)$$

where $\dot{R}$ and $\ddot{R}$ are the velocity and the acceleration of the bubble wall; σ and ν are surface tension and kinematic viscosity of the fluid; ρ_w and c_w are the fluid density and sound velocity in the water; P_g and P_o are the gas and ambient pressures; the acoustic field is given by $P_a(t) = P'_a\sin(w_a t)$, where w_a is the acoustic frequency. For the gas pressure P_g, we consider the van der Waals adiabatic equation of state:

$$P_g=\frac{P_o R_o^{3\gamma}}{(R^3-a^3)^\gamma}, \qquad (2)$$

where γ is the ratio of specific heats (for air, γ is 7/5), R_o is the initial radius of the bubble (which corresponds to the equilibrium radius when P'_a=0) and a is the van der Waals hard core (for air, $a = R_o/8.5$). The integral in eq. (1) corresponds to the total work done by the system. The term inside the integral which differentiates the pressure with respect to the time t corresponds to a 0th order correction of the liquid compressibility. The terms at the left correspond to the kinetic energy (substracted by a factor corresponding to the fluid compressibiltuy 1st order correction), and U is a potential energy term. The standard RP equation neglects U, and is obtained by differentiating eq. (1) with respect to the bubble radius R. Fig. 1a shows a typical radius evolution curve of the bubble obtained from the RP equation for parameters where SL has been observed experimentally [5]. In all our calculations we used the 4th order Runge-Kutta method with a step time dt equal to 10^{-12} s.

As proposed in ref. [11], in the vicinity of the bubble wall, the electric field E (due to the water polarization) is associated to the pressure gradient ∇p by the relation [11, 18]:

$$E_R=f\nabla p=f\rho_w\ddot{R} \qquad (3)$$

where f is the flexoelectric coefficient (for water, f has been estimated to be approximately 10^{-7} Vm^2/N [11]). In Fig. 1b we depict resulting electric fields E for two cases where SL has been observed experimentally (dashed and solid line correspond to parameter

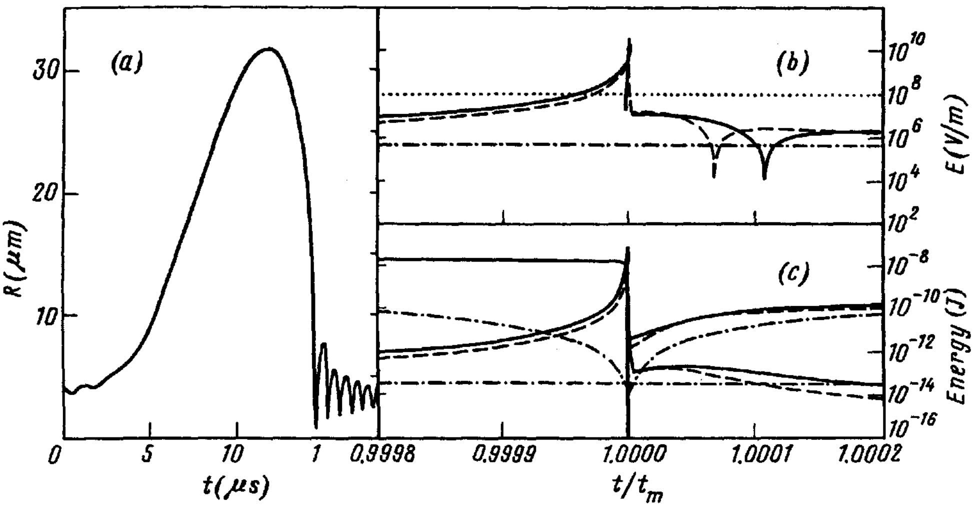

Fig.1. Solution of the RP equation (where U is neglected), for $P_a' = 1.45$ atm, $w_a/2\pi$=40 kHz and $R_o = 4\mu$m (solid curves). (a) Bubble radius R, (b) electric field E and (c) kinetic (black curves) and flexoelectric energy (gray curves) U, as a function of time t. For $P_a' = 1.45$ atm, $w_a/2\pi$=40 kHz and $R_o = 4\mu$m (solid curves); $P_a' = 1.375$ atm, $w_a/2\pi$=26.5 kHz and $R_o = 3.25\mu$m (dashed curves), and $P_a' = 1.075$ atm, $w_a/2\pi$=26.5 kHz and $R_o = 10.5\mu$m (dot-dashed curves). In (b) the horizontal dotted line corresponds to E_{bd}. In all our calculations we considered a viscosity $\nu = 0.001$ kg.m/s and a surface tension $\sigma = 0.07275$ N/m as extracted from a Handbook

conditions of ref. [4] and ref. [5], respectively). The dot-dashed curve corresponds to parameter conditions of an experiment where no SL has been observed [4]. Note that only in the two first cases, the electric field overcomes the typical electric breakdown E_{bd} of water (which is denoted by the horizontal dotted line), and this occurs before to $t/t_m = 1$, this is before the bubble reaches its minimum radius R_m at a time $t = t_m$.

The acceleration at any distance r (from the bubble center and bigger than R) is:

$$\ddot{r} = \frac{\ddot{R}R^2 + 2R\dot{R}^2}{r^2} - \frac{2R^4\dot{R}^2}{r^5} \tag{4}$$

and the potential electric energy in volume units is $U_v(r) = \frac{\epsilon_o\epsilon}{2}E(r)^2$. Therefore, the energy U reads:

$$U(R,\dot{R},\ddot{R}) = \int_R^\infty U_v 4\pi r^2 dr = 2\pi f^2 \rho_w^2 \epsilon_o \epsilon R^3(\ddot{R}^2 + 3\frac{\dot{R}^2}{R}\ddot{R} + \frac{18}{7}\frac{\dot{R}^4}{R^2}), \tag{5}$$

where ϵ_o and ϵ is the permittivity in vacuum and the dielectric coefficient of the water.

We computed the RP equation (eq. (1) for $U = 0$), and eq. (5) to estimate the flexoelectric energy U by considering $f = 10^{-7}$ Vm^2/N. We found that, for parameters where SL has been observed experimentally (same parameters as in Fig. 1b, the energy U (dashed and solid gray curves in Fig. 1c reaches values of the same order of the kinetic ones (dashed and solid black curves in Fig. 1c at the vicinity of the collapsing region ($t/t_m \sim 1$) where very high accelerations ($\sim 10^{13}$ m/s^2) take place, in contrast to the non SL case (dot-dashed curves). This indicates that in SL conditions the energy U should not be neglected as in the RP equation. In the bubble rebound ($t > t_m$), the work term due to the gas compression dominates over other terms due to the liquid. The bubble responds by increasing its radius up to the next maximum. In general, for $t > t_m$, the bubble evolution takes place with a small amount of kinetic energy and a negligible flexoelectric energy because both, the velocity and the acceleration, in the oscillating regime are much smaller than those values just before the first rebound; and the electric field does not overcome the breakdown field E_{bd} until the first rebound of the next cycle.

When considering $U \neq 0$, the largest derivative order in eq. (1) is contained in U (see eq. (5)). For this reason, at each iteration we computed R, $\dot{R}$ and $\ddot{R}$ from (1). After that, the resulting quantities are introduced in (5) to compute U for a next iteration. This procedure avoids numerical problems (for example, numerical indeterminations for $f \to 0$). Note that, we do not differentiate the equation of motion with respect to R as is done to obtain the RP equation; in this manner, the energy conservation (even in the collapsing region) is absolutely insured. Because here, $\dot{R}$ has been calculated from the quadratic velocity term (corresponding to the kinetic energy in (1)), an inconvenience appears in the choice of the velocity sign. In our case, since U is negligible for $t < t_M$ (t_M is the time where the radius bubble has a maximum -the time limiting the bubble expansion and contraction) and for $t > t_m$ (this is, after the first rebound of the bubble), we computed the different dynamical quantities of these regimes in the standard way of solving the RP equation (neglecting U); while in the bubble contraction region, the negative solution for the velocity has been considered when computing eq. (1). Furthermore, in order to take into account the energy emission mechanism when E overcomes E_{bd}, we subtracted U (which is the energy stored in water by its polarization) to the total energy accumulated in the system at each time when $E > E_{bd}$ (here, we considered E_{bd}=10^8 V/m). After that, the algorithm continues by going on to a next iteration in the calculation of eq. (1). In this work, the released energy U_r is defined as the value of U, but we point out that the results are almost the same if one considers a quantity of released energy U_r slightly smaller than U [19].

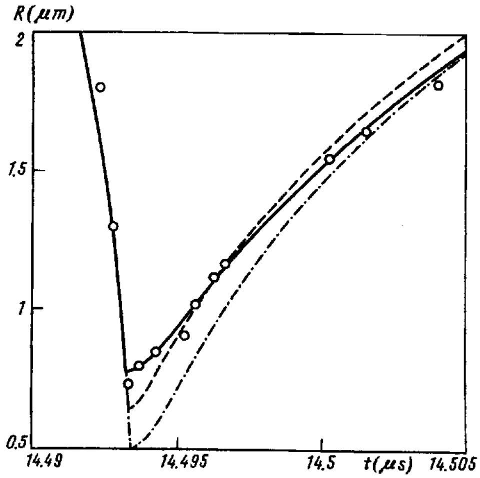

Fig.2. $R(t)$ curves for $P'_a = 1.45$ atm, $w_a/2\pi$=40 kHz and $R_o = 4\mu$m, and for $f = 0$ (dot-dashed curve), $f = 5 \cdot 10^{-8}$ (dashed curve) and $f = 10^{-7}$ (solid curve) Vm^2/N. The circles correspond to experiments of ref. [5]

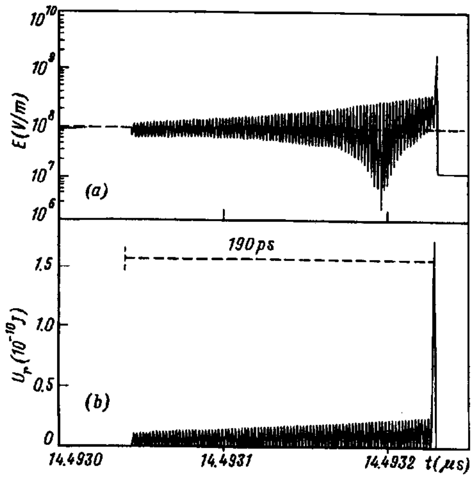

Fig.3. For same parameters as in (2) and $f = 10^{-7}$. (a) Time distribution of the electric field $E(t)$, and (b) of the released energy $U_r(t)$. For same parameters as in Fig. (2) and $f = 10^{-7}$ Vm^2/N. In (a) the horizontal dashed line indicates the considered E_{bd}

In Fig. 2 we compare $R(t)$ results obtained from RP equation ($f = 0$, dot-dashed curve), with two cases resulting when considering $U \neq 0$ in eq. (1), for $f = 5 \cdot 10^{-8}$ Vm^2/N (dashed curve) and 10^{-7} Vm^2/N (solid curve). Note that the minimum radius R_m increases with f, while for $f = 0$, R_m is a value very close to the air hard core ($R_o/8.5 \sim 0.47\mu$m). The circle symbols in Fig. 2 correspond to the experimental data that we extracted from the collapsing region of Fig. 4 of ref. [5]. The agreement between the theoretical curve for $f = 10^{-7}$ Vm^2/N and the experimental ones is quite good, in contrast to the RP case. We recall that in different SL experiments R_m resulted $\sim$0.7 μm as in our theoretical curve. For $f = 10^{-7}$ Vm^2/N the electric field E overcomes E_{bd} for the first time at a radius R_{bd} ($\sim 1.01\mu$m) bigger than R_m and at a time $t_{bd} < t_m$. At $t = t_{bd}$ the velocity $\dot{R}_{bd}$ is equal to 1159 m/s. For an estimation of the Mach Number (MN) relative to the speed of sound c_g of the gas bubble (MN=$\dot{R}/c_g$), it should be noticed that c_g depends on R, since the gas density ρ_g increase as $\rho_{g_o}(R_o/R)^3$ (ρ_{g_o} is the air density at room temperature and ambient pressure, this is 1.161 kg/m^3); i.e. for $R \sim 1.01\mu$m, $\rho_g \approx 70$ kg/m^3 (this is, $62\rho_{g_o}$, or else $0.07\rho_w$). Considering the formula of c_g for an ideal gas and the expression of the gas temperature deduced from the van der Waals theory [19], at this gas density, it results that $c_g \approx 803$ m/s ($c_g \approx 2.5c_{g_o}$). Therefore, at the beginning of the electric breakdown MN is approximately 1.44, which is a value close of MN at $R = R_m$, since in this region it results that c_g and $\dot{R}$ increases in a similar way.

An interesting point is that, when considering a breakdown field equal to 10^7 V/m and $f = 5 \cdot 10^{-8}$ Vm^2/N (parameters for which also the experimental curve is reproduced), at the moment that the first electric breakdown (this is, at radius R_{bd}) occurs, MN is 0.96 [19]. This means that the electric breakdown phenomenon may take place before the bubble wall becomes supersonic. Additionally, in the different cases discussed here, at the radius R_{bd} the gas temperature results approximately 800 K. In other words, this electrical phenomenon may take place before than other possible effects evoked in the literature to explain the SL phenomenon, like those associated to thermal effects [20, 21], those corresponding to an ingoing shock wave that passes through the center of the bubble [21], or other based on an electrical discharge in which numerous small, charged liquid jets penetrate the interior of the bubble during its collapse [22].

Fig. 3 – topshows the evolution of the electric field $E(t)$ (solid line) around the collapsing region for $f = 10^{-7}$ Vm^2/N and $E_{bd} = 10^8$ V/m (as indicated by the horizontal dashed line). As a consequence of the energy released, the $E(t)$ curve exhibits many jumps going from values where the quantity E_{bd} is exceeded to values where does not. Indeed, due to the bubble radius motion and the energy emission, the system is electrically charged and discharged. The corresponding time distribution of the energy released is illustrated in the bottom figure. As expected, the jumps are also evidenced in the $U_r(t)$ curve. Note that this emission exists in approximately 190 ps, and the quantity of released energy at each burst increases with time from approximately 10^{-11} to 10^{-10} J. In general, the increase of $U_r(t)$ with t is smooth, excluding at the end of the emission, which reveals the abrupt change of energy conditions as a prelude for the rebound of the bubble. The total energy released is 10^{-9} J per cycle, a value much bigger than the 10^{-12} J measured in SL experiments [6]. This suggests that, the efficiency of the light emission in experiments is much smaller than the unity ($\sim 10^{-3}$), and may be the remainder energy is released in other ways.

With our model we do not intend to exclude other phenomena at the moment of liberating energy, i.e. a more complicated relaxation mechanism at the moment of the electric breakdown, or other simultaneous physical phenomena produced by supersonic motions. Even if the electric breakdown phenomenon in water is of electronic character, it is difficult to clarify what happens when the energy is released, since water has a fast molecule orientation relaxation which is not accounted for by our model. On the other hand, it is possible that just at the first moment when the energy starts to be released, the system may respond with other mechanisms, which is not described by the standard hydrodynamic equations. Of course, the mechanism responsible for the relaxation may interfere strongly in the bubble motion avoiding (or, may be, allowing) supersonic wall bubble motion, but this is an open problem which should be considered for further development of our model. Unfortunately, from the experimental point of view, velocity measurements are very poor since they are obtained by measuring the slope between very few points near the minimum radius[5]. In any case, it should be noticed that the experimental maximum velocity reached by the wall bubble has been estimated to be 1200-1600 m/s [5], which corresponds to a MN of 4-6 relative to the speed of sound at room temperature and ambient pressure; while the real MN is slightly larger than 1, when considering the velocity of sound for the real density of the gas bubble. For very small radius (close to the hard core) the velocity of sound of the bubble is a value very close of that of the liquid.

In conclusion, we have presented an equation of motion for a gas bubble where the energy emission is accounted for. As was shown in this work, with the calculation of the electric field we are able to establish the electric breakdown field phenomenon as a criterion for SL, since the electric field overcomes the typical electric breakdown field in water only in those cases where SL has been observed experimentally. A very important point is that, consideration of the flexoelectric energy in the equation of motion leads to a minimum radius value which fit quite well the experimental data of refs. [4, 5], in contrast to the RP equation where resulting minimum radius is a quantity very close to the radius gas hard core. Values of duration of light emission and quantity of released energy are consistent with experiments. The breakdown may occur in water as well in the gas inside the bubble; besides, the gas polarization may explain the effects of the noble gas doping [7, 8] by the influence of the concentration gradients which also produce polarization and the influence on the breakdown voltage of minute noble gas impurities which is known since long ago as the Penning effect [23]. A non sphericity of the bubble, or a breakdown starting in a region (not at the same time in all the system), will lead to light emission with a "dipolar component" in the angular distribution of the intensity. Large magnetic fields should also modify the SL conditions because they influence the electronic motion and consequently the breakdown conditions.

We thank A.P. Levanyuk, E. Medina and P.A. Serena for helpful discussions. This study was supported by Spanish agencies and EC through the ESPRIT projects. One of us (A.H.) would like to acknowledge financial support from EC through the HCM program.

---

1. N.Marinesco and J.J.Trillat, Proc. R. Acad. Sci. **196**, 858 (1933); H.Frenzel and H.Schultes, Z.Phys.Chem. **27B**, 421 (1934).
2. D.F.Gaitan, L.A.Crum, R.A.Roy, and C.C.Church, J. Acoust. Soc. Am. **91**, 3166 (1992).

3. R.G.Holt and D.F.Gaitan, Phys. Rev. Lett. **77**, 3791 (1996).
4. B.P.Barber and S.J.Putterman, Phys. Rev. Lett. **69**, 3839 (1992).
5. K.Weninger, B.P.Barber, and S.J.Putterman, Phys. Rev. Lett. **78**, 1799 (1997).
6. R.Hiller, S.J.Putterman, and B.P.Barber, Phys. Rev. Lett. **69**, 1182 (1992).
7. R.Hiller, K.Weninger, S.J.Putterman, and B.P.Barber, Science **266**, 248 (1994).
8. R.Hiller, S.J.Putterman, and K.Weninger, Phys. Rev. Lett. **80**, 1090 (1998).
9. L.Rayleigh, Phil. Mag. **34**, 94 (1917).
10. M.Plesset, J. Appl. Mech. **16**, 277 (1949); B.Noltingk and E. Neppiras, Proc. Phys. Soc. London **B63**, 674 (1950).
11. N.García and A.P.Levanyuk, JETP Lett. **64**, 907 (1996).
12. A.K.Tagantsev, Usp.Fiz.Nauk **152**, 423 (1987) [Sov.Phys.Usp. **30**, 588 (1987)].
13. P.Harris and H.-N.Presles, J. Chem. Phys. **77**, 5157 (1982).
14. J.B.Hasted, Prog. Diel. **3**, 103 (1961).
15. Y.Toriyama and U.Shinohara, Phys.Rev. **51**, 680 (1937).
16. C.A.Sacchi, J. Opt. Soc. Am. **B8**, 337 (1991).
17. C.Herring, OSRD Rep. No. 236 (1941); A.Prosperetti and A.Lezzi, J. Fluid. Mech. **168**, 457 (1986).
18. Ya.I.Frenkel', Zhur. Fiz. Khim. **14**, 305 (1940). G.L.Natanson, Dokl.Akad.Nauk SSSR **59**, 83 (1948); M.Degrois and P.Baldo, Ultrasonics **12**, 25 (1974); M.A.Margulis, Zhur.Fiz.Khim. **59**, 1497 (1985) [Russ.J.Phys.Chem. **59**, 882 (1985)]. Ultrasonics **30**, 152 (1992).
19. A.Hasmy and N. García (to be published).
20. E.B.Flint and K.S.Suslick, Science **253**, 1397 (1991); V.Kamath and A.Prosperetti, J. Acoust. Soc. Am. **94**, 248 (1993); L.A.Crum and T.J.Matula, Science **276**, 1348 (1997).
21. C.C.Wu and P.H.Roberts, Phys. Rev. Lett. **70**, 3424 (1994); W.C.Moss, D.B.Clarke, and D.A.Young, Science **276**, 1398 (1997).
22. T.Lepoint, D. De Pauw, F.Lepoint-Mullie et al., J. Acoust. Soc. Am. **101**, 2012 (1997).
23. F.M.Penning, Naturwiss. **15**, 818 (1927); Physica **1**, 1007 (1934).